ISSN 0554-6397
UDK: 004.032.26
Original scientific paper
Received: 11th March 2022.

Ivan Ćatipović
E-mail: ivan.catipovic@fsb.hr
Katarina Martić
E-mail: km207170@stud.fsb.hr
Neven Alujević
E-mail: neven.alujevic@fsb.hr
Smiljko Rudan
E-mail: smiljko.rudan@fsb.hr
University of Zagreb, Faculty of Mechanical Engineering and Naval Architecture, Ivana Lučića 5, 10000 Zagreb, Croatia

Hydrodynamic Forces and Reactions of Two Floating Bodies in Close Proximity

Abstract

The engineering problem of two floating bodies in close proximity occurs in the case of a floating natural liquefied gas terminal when the gas is transferred from a gas carrier to a gas storage and regasification unit. An integral part of the design of such a terminal is the calculation of loads due to the incident waves. The calculation includes the assessment of first order wave forces as well as hydrodynamic reactions i.e. the added mass and the radiational damping. The calculation is based on potential flow theory with the use of three-dimensional boundary element method. Compared to the case of one floating body, the case of two bodies is more complex because it contains 12 degrees of freedom i.e. 6 degrees of freedom for each body. Therefore, the hydrodynamic coefficients and the incident waves forces must contain the interaction of the floating bodies which are in close proximity. The paper presents the results of calculations, done for two barges, which contain transfer response functions and significant force values for given sea conditions.

Keywords: floating bodies in close proximity, hydrodynamic forces, hydrodynamic reactions, boundary element method, potential flow

1. Introduction

An estimation of the seakeeping characteristics of a vessel is important to determine the operability of the vessel itself and to achieve the required level of safety at rough seas. Such estimation is based on the motion equation of a floating body derived using Newton's second law where external loads are balanced with inertial forces, [1]. The sea

state is described as a random process whose characteristics are determined by spectral analysis. The seakeeping estimations are usually done for one floating body only. The aim of this paper is to present the estimation conducted for two floating bodies that are in close proximity and are in mutual hydrodynamic interaction.

The motivation for this paper is found in floating LNG terminal (Liquified Natural Gas) and in the application of FSRU (Floating Storage and Regasification Unit). In fact, a particular situation that occurs when the terminal is used i.e. the transhipment of liquefied gas from the LNG carrier to FRSU, [2], is considered. This is done for a side-by-side configuration so that the LNG and FSRU are in close proximity, [3]. In this case there is strong hydrodynamic coupling that cannot be ignored, [4]. This coupling is manifested in forces due to incident waves but also in hydrodynamic reactions (added mass and radiational damping).

The proper evaluation of hydrodynamic forces and reactions are essential for analysis of the mooring system used at the terminal. There are two types of analyses that are currently being used: static and dynamic analysis. The static analysis assumes that all environmental forces are constant. The average values of wind and sea current are applied to calculate loads on hulls of given vessels. The wave forces are also averaged but in a particular way. When considering the loads due to waves there are the so-called first-order and second-order wave forces. The first-order wave forces are characterised by the same frequencies as the incident waves while the second order forces have frequencies that are much lower i.e. their frequencies can be determined as differences in the frequency of the incident waves. Both wave forces have zero average and therefore are neglected. However, the second order forces also contain a constant value which is included in the static analysis and can be considered as an average wave load in such type of analysis. Finally, the mooring lines loads are evaluated for total (constant) environmental load and consequently the obtained mooring loads are also constant in their values.

Downside of such a static analysis is that higher values of safety coefficient are required when choosing ropes and chains, [5]. Also, the fatigue life of mooring elements cannot be estimated. To overcome these shortcomings, the dynamic analysis is applied where all environmental loads can be considered as time-varying. The mooring loads are evaluated trough the coupled model where the motion equation is supplemented with the mooring line forces acting on the hulls of observed vessels. Mooring loads obtained in such way can be used for assessment of the fatigue life and when choosing ropes and chains the relatively lower values of safety factors can be applied (in comparison to the static approach). Here it is important to calculate wave forces that consider the hydrodynamic coupling of two floating bodies (in close proximity).

The hydrodynamics of bodies in close proximity was studied in [6] on a special case of the two identical box-shaped bodies. The developed numerical model was based on the potential theory which was solved directly in the time domain. The strong hydrodynamic coupling (between bodies) was established. Comparisons with the frequency domain results verified that the time domain method was efficient. Another

study done in the time domain was presented in [7]. Besides the hydrodynamic coupling, the mechanical coupling effects between the floating bodies due to interconnections were included in the analysis. One of the findings was that the hydrodynamic coupling had significant effect on the loads exerted on the connection system. The system was studied in more detail in [8] through the nonlinear coupling model that was calibrated by a series of model tests. It was proven that the stiffness and the pretension of the connection system had notable influence on the relative motions of the observed bodies. The relative motions of the first order of a side-by-side moored floating structures were investigated in head seas in [9]. The loads on the mooring lines and fenders was observed as well. The tensions of the mooring lines were highly dependent of the positions where the line is attached to the vessel. The line stiffness was also playing significant role in the tensions. The hydrodynamic responses of three barges in a floatover operation was investigated under various sea conditions in [10]. In conduced numerical calculations and experimental measurements, the wave shielding effect was observed. In beam sea conditions, the motions of the barge on the weather side of the wave were much larger than those of the barge on the leeside.

During side-by-side offloading operations there is a gap between the floating bodies, [11]. For example, between FSRU and LNG carrier, during offloading, the gap can be approximately 5 m. That relatively narrow gap between the vessel's hulls may be excited in resonant oscillatory wave elevations under certain wave conditions. The resonance causes certain difficulties in the numerical approaches used for the evaluation of floating bodies wave loads and motions. In the nearby region of the resonance frequency poor agreement is found in comparison with experimental results. [12] So called the pumping mode (in the gap) may cause large motions. Especially the sway motions are affected and in the case of two vessels these motions are much larger than for a single case body [13]. Also, the gap amplifies the wave loads, both the first and the second order [14].

The theory and numerical models developed in the recent studies, described above, are used in this work for evaluations od hydrodynamic properties of two floating bodies. The work is focused on the first order hydrodynamics of two rectangular barges in close proximity. So, the paper gives detailed and systematic representation of the added mass, the radiational damping and the (first-order) wave forces for the barges. Such representation is important from an engineering point of view since it gives a detailed example on how deal with the wave forces and motions of a facility like floating LNG terminal recently built at island of Krk. The example calculations are done for the barges that were studied experimentally, [15]. The theoretical background that is being used in the paper is briefly described. All the calculations are conducted for a set of regular waves. For the wave forces, one irregular wave is considered too, and significant values of these forces are evaluated. Also, the paper points out some difficulties that a designer encounters when using the described numerical approach. These difficulties are related to the resonant fluid elevation that occurs in the gap between floating bodies. The resonance is causing overestimation in calculated wave

forces and hydrodynamic reactions which is important to consider when designing facilities that involves two floating bodies.

2. Mathematical model

2.1. The motion equation

A body oscillating on a wave is in the dynamic equilibrium defined by Newton's second law. The equation of motion of a floating rigid body with 6 degrees of freedom (DOF) of motion is defined by this law in the form, [1,16].

$$\left([M]+[A]\right)\{\ddot{\eta}\}+[B]\{\dot{\eta}\}+[C]\{\eta\}=\{f\} \tag{1}$$

where are:
$[M]$ – mass matrix due to own mass
$[A]$ – added mass matrix
$[B]$ – radiational damping matrix
$[C]$ – hydrostatic stiffness matrix
$\{\ddot{\eta}\}$ – accelerations vector
$\{\dot{\eta}\}$ – velocities vector
$\{\eta\}$ – displacements vector
$\{f\}$ – excitation forces vector

In the above equation, the first part (at the left side) represent the inertial forces that are caused by the own mass of the body and the added mass. The added mass part is used to represent the inertial forces caused by the surrounding fluid (i.e. sea water) while the body is moving with a certain value of acceleration. The second part, that is proportional to the velocity, contains the damping forces. The third part are the hydrostatic forces due to the buoyancy and the weight of the floating body. Right hand side contains forces due to the incident wave considering only the first order forces.

The motion eq. (1) is a system of six linear second order differential equation (since is assumes that floating body moves in 6 DOF). For such system an assumption of harmonic body motions can be used. The harmonic motions then can be represented in complex form as

$$\{\eta\}=\{\delta\}\ \mathrm{e}^{i\omega t} \tag{2}$$

where ω is the wave frequency and $\{\delta\}$ is the complex amplitudes vector of the body motions. Whit such assumption the motion equation takes a form a complex algebraic system

$$\left(\left[C\right]-\omega^2\left(\left[M\right]+\left[A\right]\right)+\mathrm{i}\omega\left[B\right]\right)\left\{\delta\right\}=\left\{F\right\} \tag{3}$$

Here the wave forces also have a complex form as

$$\left\{f\right\}=\left\{F\right\}\ \mathrm{e}^{i\omega t} \tag{4}$$

where $\left\{F\right\}$ is excitation forces amplitudes vector.

In comparison to a single body problem, the two floating body problem is somewhat more complex because it contains 12 DOF i.e. 6 DOF for each body, Figure 1. Hydrodynamic coefficients like added mass, radiational damping as well as wave forces must contain interactions caused by a proximity of the two bodies. In this case the overall motion equation is defined by a set of 12 equations in the form, [8]

$$\left(\begin{bmatrix} C^a & 0 \\ 0 & C^b \end{bmatrix}-\omega^2\begin{bmatrix} M^a+A^{aa} & A^{ab} \\ A^{ba} & M^b+A^{bb} \end{bmatrix}+\mathrm{i}\omega\begin{bmatrix} B^{aa} & B^{ab} \\ B^{ba} & B^{bb} \end{bmatrix}\right)\begin{Bmatrix} \delta^a \\ \delta^b \end{Bmatrix}=\begin{Bmatrix} F^a \\ F^b \end{Bmatrix} \tag{5}$$

where:

M^a – mass matrix of *body-a*

A^{aa} – added mass matrix of *body-a*

B^{aa} – radiational damping matrix of *body-a*

C^a – hydrostatic stiffness matrix of *body-a*

δ^a – motions amplitude vector of *body-a*

F^a – excitation forces amplitudes vector of *body-a*

By analogy, the values defined for *body-b* are marked with ^{b} or ^{bb}. The hydrodynamic interaction between *body-a* and *body-b* is contained in matrices denoted with ^{ab} or ^{ba}. So, matrices A^{ab} and A^{ba} represent the coupling of inertial forces between the bodies. The inertial forces on *body-a* that are caused by accelerations of *body-b* are determined using matrix A^{ab} and vice versa by matrix A^{ba}. Similarly, matrices B^{ab} and B^{ba} model the coupling due to the radiational damping.

The coupling is not contained in the ^{ab} and ^{ba} matrices only. For example, matrix A^{aa} is formatted as a link between the inertial forces of the fluid acting on *body-a* caused by the accelerations of the same body. However, matrix A^{aa} considers the close presence of the *body-b* since the fluid flow around *body-a* is certainly influenced by *body-b*. Similarly, when the force amplitudes F^a and F^b are to be obtained, the fluid flow around both bodies should be taken into account. So, the coupling is also present in the wave forces.

However, hydrostatic forces are not coupled. Each body has its own buoyancy and weight that is not interconnected with other body in any way. Therefore, the non-diagonal matrices of the total hydrostatic stiffness matrix are equal to zero.

2.2. Determination of hydrodynamic components

Determination of hydrodynamic components like added mass, radiational damaging and wave forces in Eq. (3) or Eq. (5) is based on potential flow theory. This flow is non-viscous, irrotational, incompressible and homogeneous, and it is assumed that there are no cavitation gas bubbles in the fluid, [17]. The velocity potential Φ, that describes a flow around one or more floating bodies due to incident wave, is governed Laplace equation

$$\frac{\partial^2 \Phi}{\partial x^2} + \frac{\partial^2 \Phi}{\partial y^2} + \frac{\partial^2 \Phi}{\partial z^2} = 0 \tag{6}$$

The procedure for solving this equation for the case of a floating body is divided into two parts. The first part is based on the model of a fixed body on an incident wave i.e. it is assumed that the wave, although incoming, does not cause the body to move, [16,17]. The flow in this case is described by the sum of two potentials: the potential of the incident wave and the potential of its diffraction component

$$\Phi(x,\, y,\, z;t) = \Phi_0(x,\, y,\, z;t) + \Phi_7(x,\, y,\, z;t) \tag{7}$$

In addition to the Laplace equation, this sum of potentials must satisfy the boundary conditions on the free surface, the seabed, and the wetted surface of the body. By satisfying all boundary conditions, and integrating the pressures on the wetted surface of the floating body, the vector of excitation forces is determined, where the dynamic component of the pressure is determined using the linearized Bernoulli equation

$$p(x,y,z;t) = -\rho \frac{\partial}{\partial t} \Phi(x,y,z;t) \tag{8}$$

where ρ is the sea water density.

It should be noted that the overall mathematical model is linear, so the frequency domain analysis may be applied. Thus, for a given wave frequency the corresponding force amplitudes are calculated and then the displacement amplitude vectors are determined using Eq. (3). This procedure is also applied to two or more floating bodies with the same assumption i.e. that the bodies are motionless, and the integration of pressure is performed for each body individually (considering fluid flow around all bodies).

The second part of determining the velocity potential is based on the model of oscillation of a body in otherwise a calm fluid i.e. the considered floating body is placed in a state of oscillation of a given frequency and amplitude for the selected degree of freedom of movement, [16,17]. In this case, the incident wave is not taken into account, but only the radiational (outgoing) wave caused by the oscillation of the body is considered. Now, the velocity potential takes the assumed form as

$$\Phi_j(x,y,z;t) = Re\left[\delta_j \ \phi_j(x,y,z) \ e^{-i\omega t}\right] \tag{9}$$

where j denotes the number of observed degree of freedom. For a single body j takes values from 1 to 6 while in two body problem from 1 to 12. Designation stands for the complex amplitude of the potential. The procedure is carried out for all degrees of freedom individually. The total potential is obtained as the sum of all these potentials. The potential thus obtained is called the radiational potential that must meet the boundary conditions specified in the first model. By applying the Bernoulli equation and integrating the pressure over the wetted surface, the total force or hydrodynamic reactions that acts on the floating body is obtained. This reaction is further broken into two components. The first component is in anti-phase with the acceleration and represents the inertial force by which the fluid acts on the body oscillating in the fluid. Based on this component, the additional mass (by exclusion) that enters equation (3) is determined. The second component, in anti-phase with velocity, gives damping forces due to the radiational waves and serves to form a radiational damping matrix. The analogous procedure is applied to multiple floating bodies with the total number of degrees of freedom considered being $6N$ where N is the body number.

Both models have an identical mathematical solution procedure based on Green's theorems, [18]. These theorems enable mapping from the fluid domain to the domain edge. The problem is solved by defining the potential using pulsating sources/sinks placed at the domain edge, [19]. The individual source is distributed over the quadrilateral area defined as S. The total potential is then obtained as the sum of the potentials of all sources in the form

$$\Phi(x,y,z;t) = \sum_{n=1}^{N_S} Q_n \ G_n(x,y,z,\xi,\eta,\zeta)\, dS \ e^{i\omega t} \tag{10}$$

where N_s is total number of sources, Q_n is the amplitude of a single source and G_n is Green's function satisfying Laplace's equation and all listed boundary conditions except the boundary condition of the wetted surface of a floating body, [17]. The ξ, η and ζ coordinates describe the quadrilateral surface during integration. The described method is known as the boundary element method or panel method. By applying this method, the boundary elements are used to model the wetted surface of the floating body. The amplitudes of the sources are determined based on the boundary condition of the impermeability of the same wetted surface.

3. Hydrodynamics of two rectangular barges

The hydrodynamic calculations are performed for two identical rectangular barges, 2.47 m long, 0.6 m wide and with draft of 0.1 m, located next to each other. The barges were studied experimentally while being linked to a carriage, [15], and numerically in,

[20]. The distance between these barges was 12 cm. The calculation set up of the barges is shown in Figure 1. Four directions of incoming waves are observed: 0^O, 30^O, 60^O and 90^O. The calculation was performed for a range of wave frequencies from 5 to 9 rad/s. The frequency step is 0.02 rad/s, so a total of 201 wave frequencies are considered. Significant values of the wave forces are obtained with ITTC wave spectrum and the significant wave height of 4 cm. Also, the fluid elevation in the gap between the barges are calculated and compared with experimental results. The software package HydroStar [21] was used for the numerical calculations. The panel layout for these barges is shown in Figure 2.

3.1. Numerical results

Graphs 1 to 6 show the obtained values of hydrodynamic reactions i.e. additional mass and radiational damping for the given wave frequencies. In more detail, the diagonal elements of the corresponding matrices are shown. The graphs show the results for the first and the second barge (located in close proximity as shown in Figures 1 and 2). For comparison, the graphs also show the results for a stand-alone barge considered as a single floating body and modelled by Eq. (3). Calculations were performed for 6 degrees of freedom for each of the considered barges, however the presented results are related only to the horizontal plane because it is assumed that the hydrodynamic characteristics of barges in this plane have the greatest impact on the mooring system, [22]. In more detail, for the calculation of the load of the mooring system, within the coupled model, only the hydrodynamic forces and reactions in the horizontal plane are usually considered, [23,24].

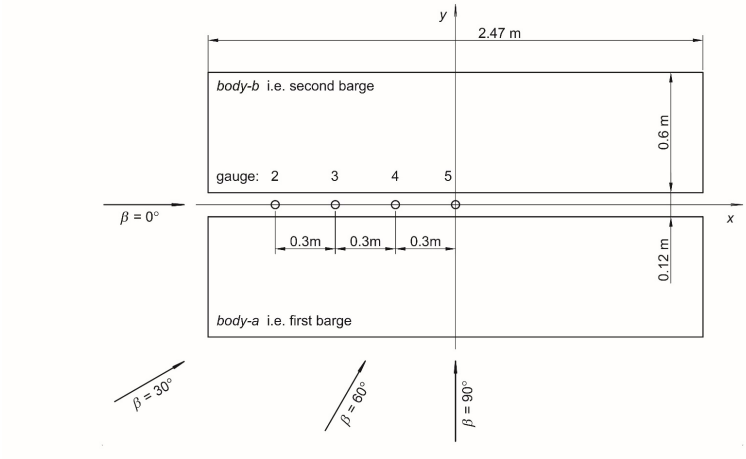

Figure 1. The location of barges and wave gauges with the indicated directions of incident waves

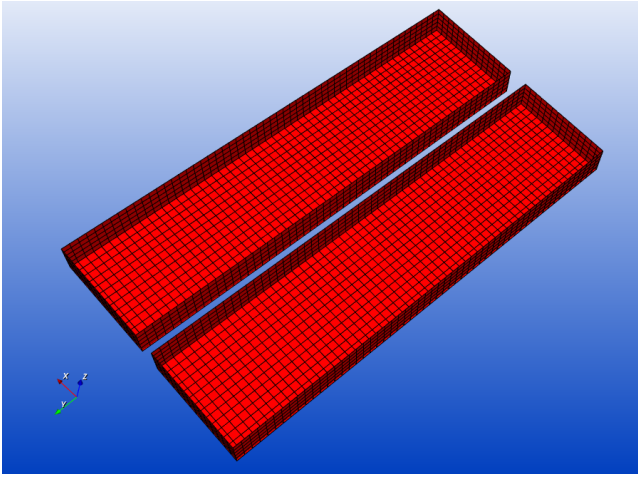

Figure 2. Panel model of the barges

Graphs 7 to 12 show the transfer functions of forces and moments in the horizontal plane. Only the directions of the incident waves of 30^{O} and 90^{O} are selected for presentation (due to conciseness in the graphical presentation of the results). The results for the stand-alone barge and the first and second barge are also presented here in parallel. It should be noted that values of the transfer function on Graphs 8 and 12 are almost zero for whole ranges of observed frequencies. This is in line with theoretical reasoning since the beam waves are considered i.e. incident wave direction is 90^{O}. Such wave direction will not cause surge forces nor yaw moments.

Table 1 shows the significant values of forces and moments for the stand-alone barge. Table 2 shows these kinds of significant values but for the first barge. This table also shows the relative deviations from the stand-alone barge. Table 3 is analogous to Table 2 and shows the values related to the second barge.

4. Discussion

A review of the above graphs can generally show a large difference between the results related to the stand-alone barge and the results related to the first or the second barge. The difference in some seakeeping characteristics is the whole order of magnitude. Peaks, or abrupt changes in the results related to the narrow range of certain frequencies, are also observed in all graphs.

The first fact clearly highlights the problem of floating bodies in the close proximity i.e. the emergence of hydrodynamic coupling, which must be taken into account when designing a mooring or anchoring system, [2]. Coupling is manifested through hydrodynamic reactions and wave forces. A contribution to this can be found in Tables

1, 2 and 3 where the deviations in the significant value of the forces and moments of the first and second barge in relation to the stand-alone barge reach approximately 250%.

Another fact suggests the existence of a resonant phenomenon in the system of two barges and the surrounding fluid. This phenomenon is known as resonant fluid elevation in the interspace between floating bodies, the so-called gap resonance, [4]. The consequence of this resonance is peaks in the transfer functions of excitation forces and moments, Graphs 7, 9, 10 and 11. Peaks are also observed in additional mass and radiational damping, Graphs 1 to 6. These peaks are more pronounced for certain degrees of freedom i.e. the peaks are more noticeable in sway and yaw and less in surge.

It should be noted that the occurrence of this resonant phenomenon can be observed in real conditions, however the amount of resonant elevation itself is significantly less than can be obtained by the presented type of numerical calculations. In real conditions, damping plays a significant role, as with all resonant phenomena, and reduces the amount of such elevation. Alternatively, there are different forms of damping that significantly reduce this elevation. Within the usual potential theory, and thus in the calculations presented in this paper, there is no corresponding mathematical model of damping for the resonant elevation. This is observed in Graphs 13 to 18 where the response amplitude operator (RAO) of the fluid elevations are shown. The two set of experimental result are obtained from [15] that are measured at the wave gauges whose positions are is shown in Figure 1. In all the graphs, the overestimated numerical values can be observed in comparison with the experimental data.

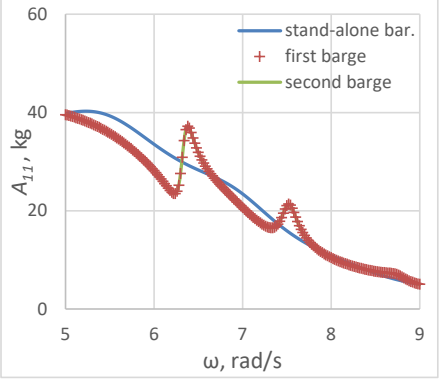

Graph 1. Surge added mass

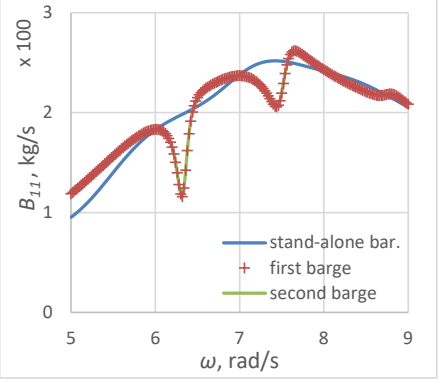

Graph 2. Surge radiational damping

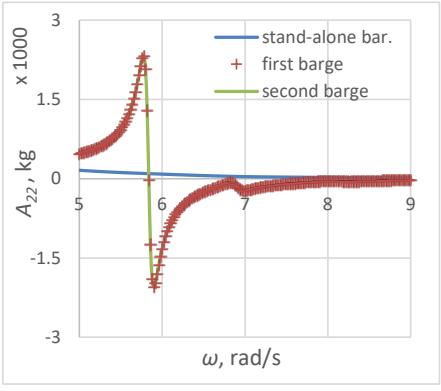

Graph 3. Sway added mass

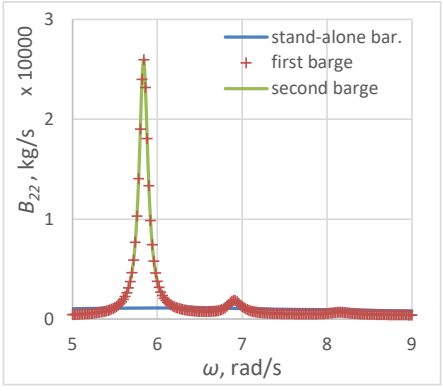

Graph 4. Sway radiational damping

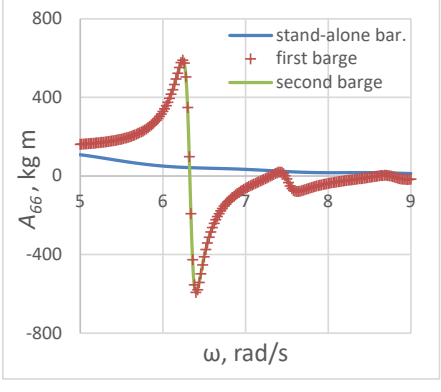

Graph 5. Yaw added mass

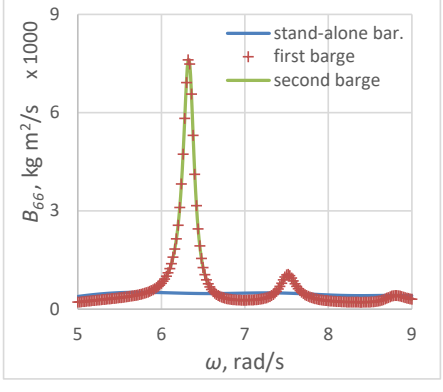

Graph 6. Yaw radiational damping

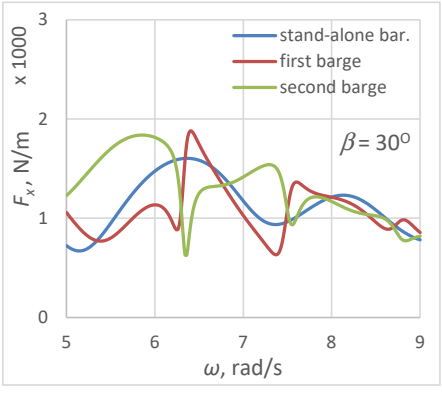

Graph 7. Surge force transfer function, $\beta = 30^O$

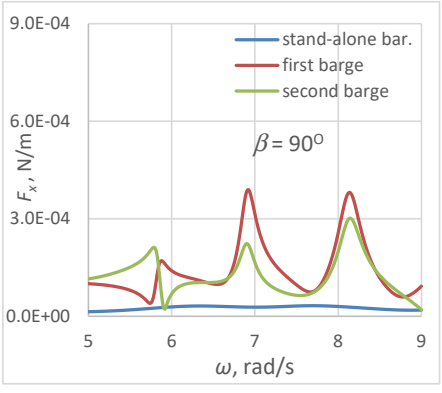

Graph 8. Surge force transfer function, $\beta = 90^O$

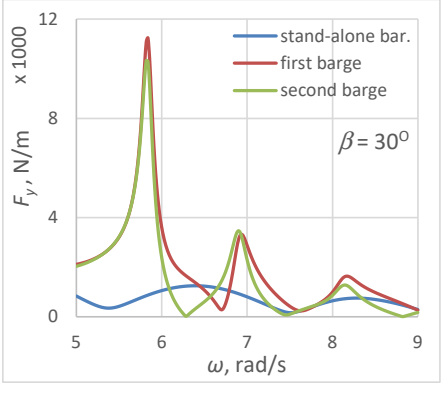

Graph 9. Sway force transfer function, $\beta = 30^O$

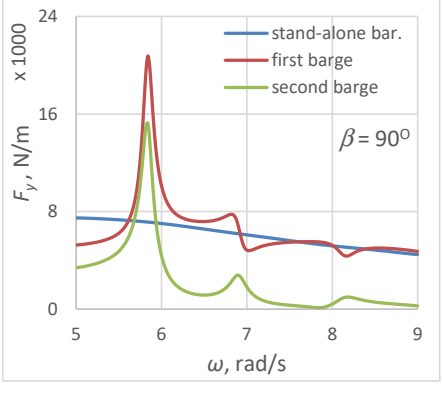

Graph 10. Sway force transfer function, $\beta = 90^O$

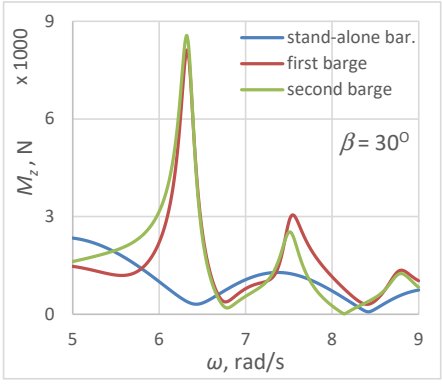

Graph 11. Yaw moment transfer function, $\beta = 30^O$

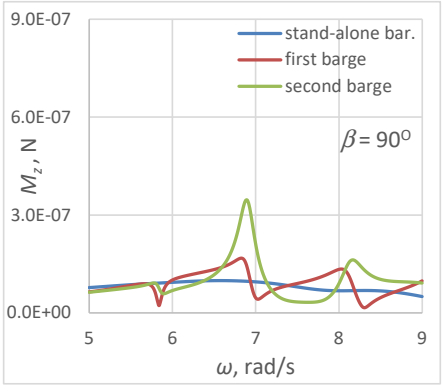

Graph 12. Yaw moment transfer function, $\beta = 90^O$

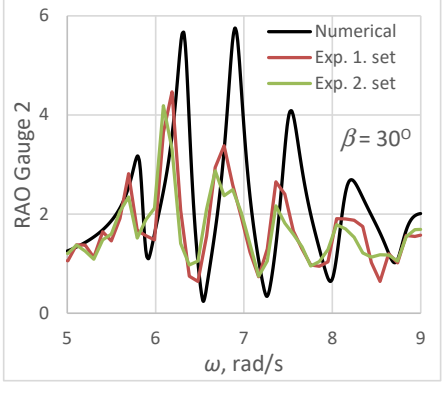

Graph 13. RAO at gauge 2, $\beta = 30^O$

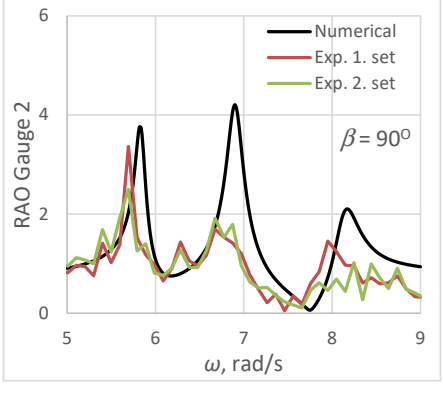

Graph 14. RAO at gauge 2, $\beta = 90^O$

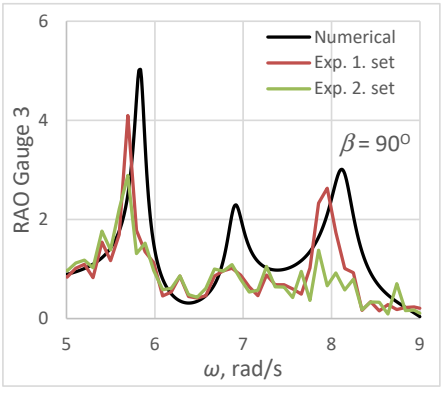

Graph 15. RAO at gauge 3, β = 90O

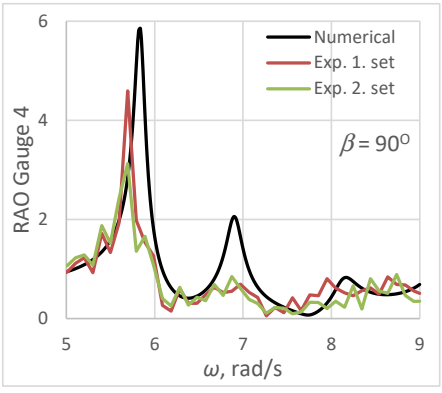

Graph 16. RAO at gauge 4, β = 90O

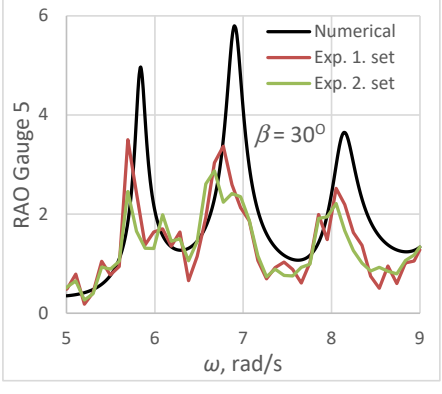

Graph 17. RAO at gauge 5, β = 30O

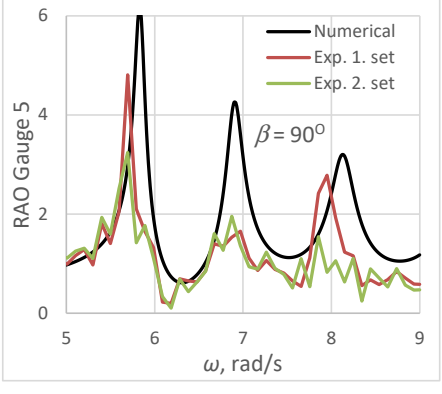

Graph 18. RAO at gauge 5, β = 90O

Table 1. Standalone barge: significant values of forces and moments

β, ^{O}	F_x, N	F_y, N	M_z, Nm
0	106.8	0.0	0.0
30	36.3	17.6	46.8
60	14.3	20.5	21.1
90	0.0	23.3	0.0

Table 2. First barge: significant values of forces and moments, deviations in relation to the standalone barge

β, ^{O}	F_x, N	F_y, N	M_z, Nm	dev. F_x, %	dev. F_y, %	dev. M_z, %
0	127.9	0.0	0.0	19.7	/	/
30	74.3	17.8	56.1	104.4	0.8	20.0
60	52.6	19.7	43.9	267.5	-3.9	108.3
90	56.0	23.0	41.5	/	-1.4	/

Table 3. Second barge: significant values of forces and moments, deviations in relation to the standalone barge

β, ^{O}	F_x, N	F_y, N	M_z, Nm	dev. F_x, %	dev. F_y, %	dev. M_z, %
0	69.7	0.0	0.0	-34.8	/	/
30	76.7	17.1	30.1	111.2	-3.1	-35.6
60	48.5	23.4	48.1	238.9	14.2	128.5
90	56.0	23.0	41.5	/	-1.4	/

However, the overestimated elevations cannot be considered as the main issue here. In general, the elevations values are not of practical engineering concern when, for example, a mooring system for LNG terminal is designed. The actual problem is in the calculated first order wave forces, that are also overestimated. The forces overestimation is a consequence of the elevations' overestimation, [4,15]. Simply put, higher elevations cause higher pressures over a hull's wetted surface so integrating these pressures leads to higher (overestimated) values of forces and moments. The same explanation can be used for the hydrodynamic reactions. This can be observed by comparisons of the graphs were the forces and elevations are presented. The frequencies where peak elevations occurred are very close to the peak frequencies of the forces

(or the moments). This is most pronounced at Graphs 9 and 17 where incident wave direction is 30^{O} and where the sway force and RAO of gauge 5 and are presented, respectively. Similar can be observed at Graphs 10 and 18. Furthermore, the relatively large deviations in the significant value of the forces and moments of the first and second barge in relation to the stand-alone barge, as presented in Table 2 and 3, are party caused by the described phenomena.

The solution that is applied in practice consist of an additional damping that is introduced through a dissipation zone that covers the interspace between two vessels in the close proximity, thus obtaining more realistic elevation and force values, [3,4]. It should also be noted that the occurrence of resonance also affects the second-order wave forces that also cause a significant load on the mooring system, [24].

5. Conclusion

In this paper, the calculations of hydrodynamic forces and reactions acting on two floating bodies i.e. two barges were performed. The results obtained point to following facts.

The first fact highlights the hydrodynamic coupling between floating bodies located in the close proximity. Coupling is manifested both in excitation forces due to incident waves and in hydrodynamic reactions (additional mass and radiational damping).

Another fact refers to the occurrence of resonant fluid elevation in the space between the two barges. In real conditions, there are various forms of damping that significantly reduce this elevation. However, commonly used calculations are based on potential theory (or on non-viscous fluid) where damping is neglected. As a result, such calculations overestimate the elevation but also the wave forces of the first order as well as the hydrodynamic reactions at resonance frequencies. In practice, the problem is overcome by introducing a dissipation zone in the interspace of floating bodies in order to obtain more realistic elevation values.

These facts should be considered when designing a mooring system. This paper presents the basic settings and an example of a calculation including hydrodynamic coupling. This is relevant from an engineering point of view since the current practice for evaluation of the mooring line tension certainly includes the hydrodynamics of moored bodies. As indicated, such approach can be used for assessment of the fatigue life. Also, when choosing ropes and chains, the relatively lower values of safety factors can be applied (in comparison to the static approach) without compromising the system safety. In the continuation of this paper, the introduction of the dissipation zone and its impact on the forces and moments that loads the mooring system should certainly be considered.

Acknowledgments

The Croatian Science Foundation HRZZ- IP-2019-04-5402 (DARS) support is gratefully acknowledged.

References

1. Čorić, V., Prpić-Oršić J.: Pomorstvenost plovnih objekata; Zigo, Rijeka, 2006.
2. Ye, W., Luo, Y., Pollack, J.: LNG floating regasification unit (FRU) side-by-side mooring analysis. 24th International Conference on Offshore Mechanics and Arctic Engineering (OMAE 2005), Halkidiki, Greece, 2005.
3. Huijsmans, R.: Advances in the hydrodynamics of side-by-side moored vessels. Proceedings of the 26th International Conference on Offshore Mechanics and Arctic Engineering (OMAE 2007), San Diego, California, USA, 2007.
4. Bunnik, T., Pauw, W., Voogt, A.: Hydrodynamic analysis for side-by-side offloading. Proceedings of the 19th International Offshore and Polar Engineering Conference (ISOPE 2009), Osaka, Japan, 2009.
5. BS 6349- Maritime Structures - Part 6: Design of Inshore Mooring and Floating Structures, British Standard Institution, London, 1989.
6. Zhu, H.R., Zhu, R.C., MIAO, G.P. (2008). A time domain investigation on the hydrodynamic resonance phenomena of 3-D multiple floating structures. Journal of Hydrodynamics, Ser. B 20 (5), 611–616.
7. Zhao, W. H., Yang, J. M., Hu Z. G. (2012). Hydrodynamic interaction between FLNG vessel and LNG carrier in side by side configuration. Journal of Hydrodynamics, Ser. B 24(5), 648-657.
8. Zhao, W.H., Yang, J.M., Hu, Z.Q., Tao, L.B. (2014). Prediction of hydrodynamic performance of an FLNG system in side-by-side offloading operation. Journal of Fluids and Structures 46, 89–110.
9. Pessoa, J., Fonseca, N., Soares, C.G. (2015). Numerical study of the coupled motion responses in waves of side-by-side LNG floating systems. Applied Ocean Research 51, 350–366.
10. Xu, X., Yang, J.M., Li, X., Xu, L.Y. (2015). Time-domain simulation for coupled motions of three barges moored side-by-side in floatover operation. China Ocean Engineering 29, 155–168.
11. Zhao, W., Milne, I. A., Efthymiou, M., Wolgamot, H. A., Draper, S., Taylor, P. H., Eatock Taylor, R. (2018). Current practice and research directions in hydrodynamics for FLNG-side-by-side offloading. Ocean Engineering 158, 99-110.
12. Hong, S. Y., Kim, J. H., Cho, S. K., Choi, Y. R., Kim, Y. S. (2015). Numerical and experimental study on hydrodynamic interaction of side-by-side moored multiple vessels. Ocean Engineering 32, 783–801.
13. Koo, B. J., Kim, M. H. (2005). Hydrodynamic interactions and relative motions of two floating platforms with mooring lines in side-by-side offloading operation. Applied Ocean Research 27, 292–310.
14. Perić, M., Swan, C. (2015). An experimental study of the wave excitation in the gap between two closely spaced bodies, with implications for LNG offloading, Applied Ocean Research, 51, 320-330.
15. Molin, B., Remy, F., Camhi, A., Ledoux, A.: Experimental and numerical study of the gap resonances in-between two rectangular barges, Congress of International Maritime Association of the Mediterranean, IMAM 2009, Istanbul, Turkey, 2009.
16. Faltinsen, O.M., Michelsen, F.C.: Motions of large structures in waves at zero froude number. International Symposium: The Dynamics of Marine Vehicles and Structures in Waves, London, England, 1974.
17. Faltinsen, O.M.: Sea Loads on Ships and Offshore Structures, Cambridge University Press, 1993.
18. Chakrabarti, S. K. (2001). Application and verification of deepwater green function for water waves. Journal of Ship Research 45(3), 187–196.
19. Wehausen, J. V., Laitone, E. V.: Surface Waves. Encyclopedia of Physics, Springer – Verlag, 1960.

20. Martić, K.: Proračun hidrodinamičkih sila na dva plutajuća tijela u neposrednoj blizini, Završni rad; Sveučilište u Zagrebu, Fakultet strojarstva i brodogradnje, Zagreb, 2016.
21. Bureau Veritas. HydroStar for Experts—User Manual; Bureau Veritas: Paris, France, 2018.
22. API RP 2SK: Design and Analysis of Stationkeeping Systems for Floating Structures, American Petroleum Institute, 3rd Edition, Washington, 2005.
23. DNV-RP-H103, Det Norske Veritas: Recommended Practice: Modelling And Analysis of Marine Operations, Høvik, Norway, 2010.
24. Bureau Veritas, Marine & Offshore Division: NR493 R03: Classification of Mooring Systems for Permanent and Mobile Offshore Units, Paris, 2015.